



ARCHIVES  
of  
FOUNDRY ENGINEERING

DOI: 10.1515/afe-2017-0063

Published quarterly as the organ of the Foundry Commission of the Polish Academy of Sciences

ISSN (2299-2944)  
Volume 17  
Issue 2/2017

125 – 130

# Effect of Sr and Ti Addition on the Corrosion Behaviour of Al-7Si-0.3Mg Alloy

M. Uludağ<sup>\*,a</sup>, M. Kocabaş<sup>b</sup>, D. Dışınar<sup>c</sup>, R. Çetin<sup>d</sup>, N. Cansever<sup>b</sup><sup>a</sup> Selcuk University, Faculty of Engineering, Metallurgical and Materials Eng. Dept., Konya-Turkey<sup>b</sup> Yıldız Technical University, Faculty of Chemistry-Metallurgy, Metallurgical and Materials Eng. Dept., Istanbul-Turkey<sup>c</sup> Istanbul University, Faculty of Engineering, Metallurgical and Materials Eng. Dept., Istanbul-Turkey<sup>d</sup> Halic University, Faculty of Engineering, Industrial Eng., Istanbul-Turkey

\* Corresponding author. E-mail address: dr.uludagm@gmail.com

Received 10.07.2016; accepted in revised form 31.10.2016

## Abstract

In the present study, the corrosion behaviour of A356 (Al-7Si-0.3Mg) alloy in 3.5% NaCl solution has been evaluated using cyclic/potentiodynamic polarization tests. The alloy was provided in the unmodified form and it was then modified with AlTi5B1 for grain refinement and with AlSr15 for Si modifications. These modifications yield to better mechanical properties. Tensile tests were performed. In addition, bifilm index and SDAS values were calculated and microstructure of the samples was investigated. As a result of the corrosion test, the  $E_{corr}$  values for all conditions were determined approximately equal, and the samples were pitted rapidly. The degassing of the melt decreased the bifilm index (i.e. higher melt quality) and thereby the corrosion resistance was increased. The lowest corrosion rate was founded at degassing and as-received condition ( $3.9 \times 10^{-3}$  mm/year). However, additive elements do not show the effect which degassing process shows.

**Keywords:** A356 alloy, Bifilm index, Grain refinement, Modification, Electrochemical corrosion.

## 1. Introduction

Among the various classes of aluminum alloys, Al-Si-Mg base alloys hold superior properties such as excellent castability, weldability, pressure tightness and corrosion resistance and are hence widely used in the aerospace and automotive industries. The applications include engine block, cylinder head, piston, wheel etc. [1, 2]. In this work, one of the most commonly used A356 (Al-7Si-0.3Mg) alloy was studied.

In order to improve the mechanical properties of these alloys, several alloying elements are added. The typical addition is Al-Ti-

B which refines the microstructure to achieve more globular, finer and homogeneously distributed dendrites [3-10]. Ultrasonic vibration has also been applied in order to refine the microstructure [11-15]. The microstructure of Al-Si alloys consists of needle like coarse Si particles which may act as stress risers. Therefore, Sr is commonly used to modify the Si particles such that finer and fibrous Al-Si eutectic microstructure can be achieved [16-18].

During casting of aluminum alloys, hydrogen has been blamed as the major source of porosity formation. However, Campbell [19] has shown that surface entrained defects, known as bifilms (Figure 1), have major effect over several properties of

cast aluminum alloys such as increased porosity formation, lowered mechanical properties etc. These bifilms may become incorporated into the melt simply by turbulent transfer or turbulent filling during casting operations. Dispinar [20-23] extensively studied the effects of bifilms and proposed a quality measurement method named as “bifilm index”.

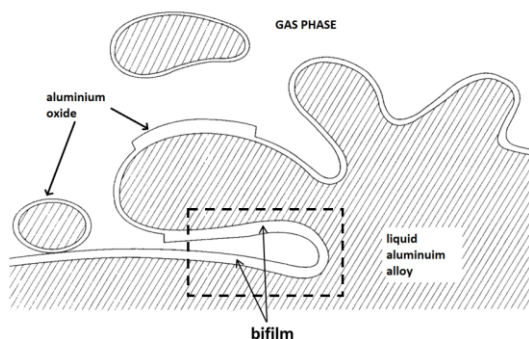


Fig. 1. Formation of bifilm by turbulence and entrainment of surface oxide [19]

Although there are some studies about the correlation between corrosion behaviour and the degassing and modification of A356 [24-26], these studies did not include the bifilm index. In this work, the effect of bifilms on the corrosion resistance of A356 alloy was investigated. The alloys were cast in three different conditions: as-received, Ti grain refined and Sr modified-Ti grain refined.

## 2. Experimental Work

### 2.1. Materials and Casting

The chemical composition of the A356 primer alloy that was used in the tests is shown in Table 1.

Table 1.

Chemical composition of A356 alloy (%)

Alloy	Si	Fe	Cu	Mn	Mg	Zn	Ti	Al
A356	6.70	0.20	0.02	0.03	0.38	0.04	0.14	Rem

15 kg of A356 charges were melted in SiC crucible in a resistance furnace at 740 °C. Degassing was carried out with Ar for 20 minutes and cylindrical bars were cast into a sand mould. The dimension and the mould geometry are given in Figure 2. In all the tests, the hydrogen content of the melt was measured by AlSpek. Degassing was carried out with Ar for 20 minutes. It was found that hydrogen level was 0.25-0.30 ml/100g Al before degassing and 0.10-0.15 ml/100g Al after degassing. Reduced pressure test (RPT) samples were collected in order to determine the quality of the melt by means of measuring bifilm index. Detailed explanation of how to measure bifilm index was given in Ref [27]. The cast samples were sectioned and subjected to metallographical examination. The microstructures of samples

were investigated by optical microscope. The cylindrical bars were machined into the specific dimension and subjected to tensile testing to determine the mechanical properties according to ASTM-E800.

The same procedure was carried out for Sr modified and Sr modified-Ti grain refined melts. The samples were collected before and after degassing. Overall, 6 different conditions were studied. The parameters of the study are given in Table 2.

Table 2.

Experimental parameters

T1	As-received and no degassing
T2	As-received and degassed
T3	AlSr15 addition and no degassing
T4	AlSr15 addition and degassed
T5	AlSr15+AlTi5B1 addition and no degassed
T6	AlSr15+AlTi5B1 addition and degassed

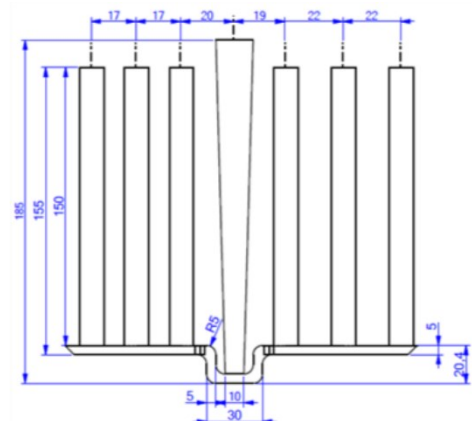


Fig. 2. a) The dimension of the mould b) Sand mould

## 2.2. Electrochemical investigation method

Potentiodynamic and cyclic polarization tests were performed to evaluate the corrosion resistance of cast samples using test solutions with 3.5% NaCl solution at room temperature. Prior to each experiment, the specimen surface was polished to 1200 grit surface finish and degreased with acetone. Also, these specimens immersed in the solution for 15 min before polarization tests. The electrochemical experimental set-up was composed of a classic three electrodes cell using a carbon rod as counter electrode and a saturated calomel electrode (SCE) as the reference one, the samples being connected to the working electrode. All the electrochemical experiments were performed by a potentiostat Gamry interface 1000 at a scanning rate of 2 mV/s. All the potentials referred in this paper are with respect to SCE.

## 3. Results and discussion

### 3.1. Alloy microstructure and composition

All the samples were subjected to metallographical examination and the microstructural images are given in Figure 3. In these images, T1 and T2 represent the microstructure of as-received alloy before and after degassing. Similarly, T3 and T4 is the alloy that was Sr modified and T5 and T6 is the Sr modified-Ti grain refined samples, before and after degassing.

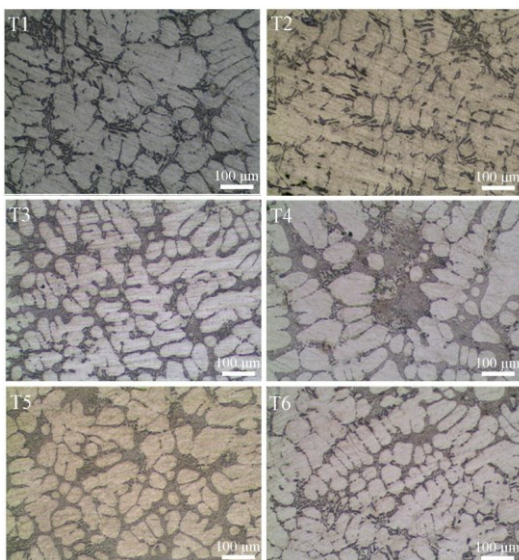


Fig. 3. The microstructures of A356 alloy for different conditions

Image analysis was carried out on the microstructures and SDAS was measured. As seen in Figure 4, the grain size of as-received, Sr modified and Sr modified-Ti grain refined castings are 42, 36 and 31  $\mu\text{m}$ , respectively.

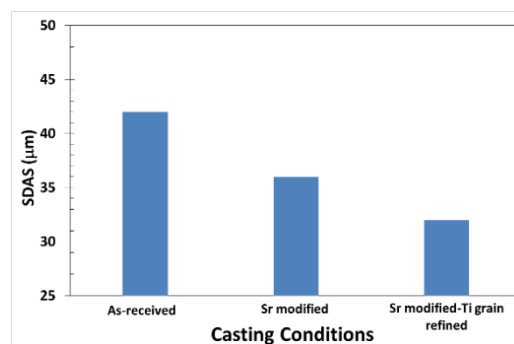


Fig. 4. Cast conditions vs. SDAS

The tensile test results of all the castings were summarized in Figure 5. As can be seen, tensile strength and elongation (%) values of the cast samples are increased by degassing process. Ultimate tensile strength of the alloy was around 167 MPa with 2% elongation on as-received and degassed alloy.

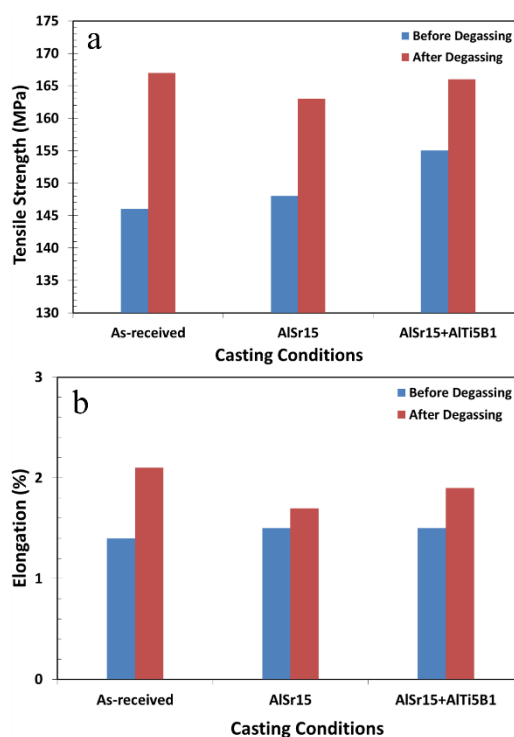


Fig. 5. Mechanical properties of A356 Al alloy a) Tensile Strength b) Elongation

### 3.2. Casting quality and hydrogen content

The bifilm index measurements were carried out from the sectioned surface of reduced pressure test samples that were solidified under 100 mbar. The results show that, before degassing of the melt, the hydrogen level was above 0.2  $\text{cm}^3/100\text{g}$  Al and the bifilm index were between 50 and 100 mm. After

degassing, the hydrogen levels were dropped down to 0.12 and bifilm index was around 15 mm.

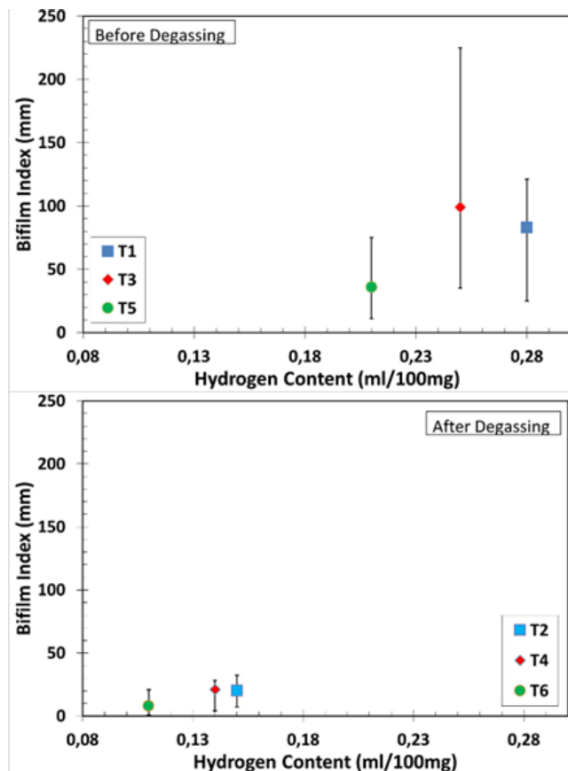


Fig. 6. Bifilm index vs. Hydrogen Content

### 3.3. Electrochemical measurements

Al and its alloys are exposed pitting corrosion in NaCl solution. However, there are limited studies in the literature about degassed, Sr modified and Sr modified-Ti grain refined A356 cast alloy in NaCl solution.

In this work, the corrosion behavior of A356 alloy was investigated under three different casting conditions; as-received, Ti grain refined and Sr modified-Ti grain refined. In order to do this potentiodynamic and cyclic polarization tests were performed with 3.5% NaCl solution at room temperature for each sample under degassed and no degassed.

Fig. 7 shows the cyclic polarization curves of A356 alloy in the no degassed samples. Fig. 8 shows the potentiodynamic polarization curves of A356 alloy under degassed conditions in 3.5% NaCl solution. In addition, Table 3 shows the electrochemical corrosion data for A356 Al alloy.

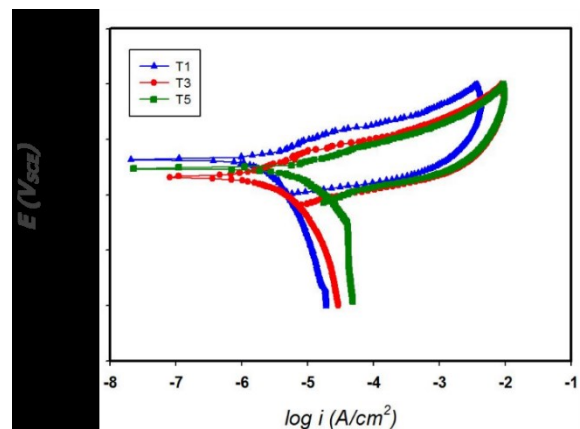


Fig. 7. Cyclic polarization curves for A356 Al alloy under no degassed in 3.5% NaCl solution

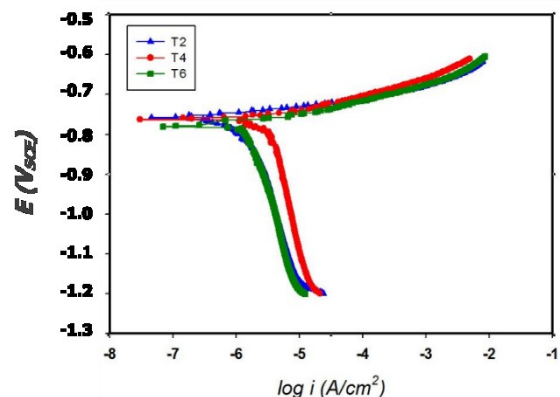


Fig. 8. Potentiodynamic polarization curves for A356 Al alloy under degassed in 3.5% NaCl solution

As can be seen in Fig. 7 and Fig. 8, the rapid increase in current density on the anodic range indicates that pitting is occurred rapidly on the samples. The rapid increase in current density on the anodic range indicated that the pitting potential,  $E_{pit}$ , was close to  $E_{corr}$  and the materials were pitting freely at the corrosion potential. As indicated by the limited current region in the cathodic branches, the corrosion process in naturally-aerated NaCl solution was found to be under cathodic control (oxygen diffusion) for alloys.

The  $E_{corr}$  values for all six conditions were determined approximately equal. However, the corrosion rates of A356 Al alloy are  $20.1 \times 10^{-3}$ ,  $3.9 \times 10^{-3}$ ,  $31.1 \times 10^{-3}$ ,  $23.4 \times 10^{-3}$  and  $66.4 \times 10^{-3}$ ,  $12.4 \times 10^{-3}$  mm/year respectively. The highest corrosion rate ( $66.4 \times 10^{-3}$  mm/year) was obtained at Sr modified-Ti grain refined A356 Al alloy under T5 conditions.

The corrosion rate was calculated by  $I_{corr}$  values and also the pitting potential ( $E_{pit}$ ) and the repassivation potential ( $E_{rep}$ ) values were obtained from cyclic polarization curves which are also shown in Table 3. The  $E_{rep}$  was below  $E_{corr}$  for all conditions, indicating favourable conditions for stable pit growth. The corrosion rate is calculated with the following equation 1;

$$\text{Corrosion Rate (mm/year)} = \frac{C \cdot M \cdot i}{n \cdot d} \quad (1)$$

Where C is constant number (0.00327), M is the atomic weight in g/mol, i is the current density in  $\mu\text{A}/\text{cm}^2$ , n is the electron number and d is the density in  $\text{g}/\text{cm}^3$  of Al.

Table 3.

Electrochemical corrosion data for A356 Al alloy

	T1	T2	T3	T4	T5	T6
$E_{\text{corr}}$ (mV)	-0.736	-0.758	-0.766	-0.762	-0.751	-0.780
$I_{\text{corr}}$ ( $\mu\text{A}$ )	1.850	0.362	2.858	2.149	6.112	1.145
$E_{\text{rep}}$ (mV)	-0.798	-0.800	-0.822	-0.860	-0.811	-0.874
$E_{\text{pit}}$ (mV)	-0.680	-0.729	-0.708	-0.728	-0.717	-0.733
Corr. rate (mm/year)	$20.1 \times 10^{-3}$	$3.9 \times 10^{-3}$	$31.1 \times 10^{-3}$	$23.4 \times 10^{-3}$	$66.4 \times 10^{-3}$	$12.4 \times 10^{-3}$

As far as  $E_{\text{rep}}$  value shows the repassivation potential of pits, narrow  $E_{\text{pit}}-E_{\text{rep}}$  potential space indicated easy repassivation of the existing pits [5]. Fig. 9 shows the difference at  $E_{\text{corr}}$ ,  $E_{\text{pit}}$  and  $E_{\text{rep}}$  values according to the different conditions. This potential values get close to each other at most under T2 and T5 conditions.

corrosion rate ( $3.9 \times 10^{-3}$  mm/year) was obtained at as-received and degassed A356 Al alloy.

## References

- [1] Chomsaeng, N., Haruta, M., Chairuangri, T., Kurata, H., Isoda, S. & Shiojiri, M. (2010). HRTEM and ADF-STEM of precipitates at peak-ageing in cast A356 aluminum alloy. *Journal of Alloys and Compounds*. 496(1), 478-487.
- [2] Tsai, Y.-C., Chou, C.-Y., Lee, S.-L., Lin, C.-K., Lin, J.-C. & Lim, S. (2009). Effect of trace La addition on the microstructures and mechanical properties of A356 (Al-7Si-0.35 Mg) aluminum alloys. *Journal of alloys and compounds*. 487(1), 157-162.
- [3] Górný, M., Sikora, G. & Kawalec, M., (2016). Effect of Titanium and Boron on the Stability of Grain Refinement of Al-Cu Alloy. *Archives of Foundry Engineering*. 16(3), 35-38.
- [4] Kori, S., Murty, B. & Chakraborty, M. (2000). Development of an efficient grain refiner for Al-7Si alloy. *Materials Science and Engineering: A*. 280(1), 94-104.
- [5] Ma, T., Chen, Z., Nie, Z. & Huang, H. (2013). Microstructure of Al-Ti-B-Er refiner and its grain refining performance. *Journal of Rare Earths*. 31(6), 622-627. 10.1016/S1002-0721(12)60331-7.
- [6] Mi, L., Wang, J.J. & Hu, Z.L., (2014). The research progress of TiB<sub>2</sub> impacts on the refining effect of Al-Ti-B master alloy. *Applied Mechanics and Materials*. 391-395.
- [7] Mohanty, P. & Gruzleski, J. (1996). Grain refinement mechanisms of hypoeutectic Al-Si alloys. *Acta materialia*. 44(9), 3749-3760.
- [8] Qiu, K., Wang, R.C., Peng, C.Q., Wang, N.G., Cai, Z.Y. & Zhang, C. (2015). Effects of Mn and Sn on microstructure of Al-7Si-Mg alloy modified by Sr and Al-5Ti-B. *Transactions of Nonferrous Metals Society of China (English Edition)*. 25(11), 3546-3552. 10.1016/S1003-6326(15)64075-4.
- [9] Timelli, G., Camicia, G. & Ferraro, S. (2014). Effect of Grain Refinement and Cooling Rate on the Microstructure and Mechanical Properties of Secondary Al-Si-Cu Alloys. *Journal of materials engineering and performance*. 23(2): range of pages.

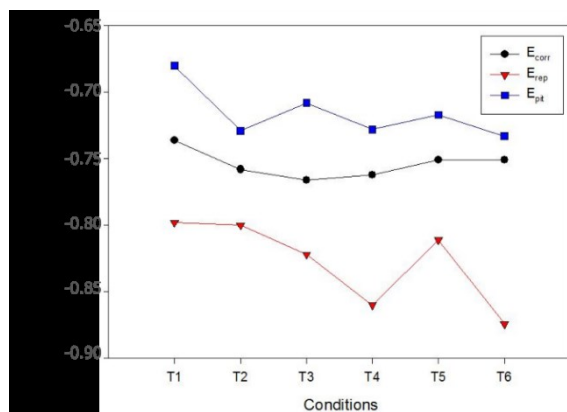


Fig. 9.  $E_{\text{corr}}$ ,  $E_{\text{pit}}$  and  $E_{\text{rep}}$  values of A356 aluminum alloys for all conditions

## 4. Conclusions

The microstructure, mechanical properties and corrosion behaviour of cast A356 aluminum alloy were examined and the following conclusions are drawn from the present study.

- Modification by Sr and Ti decreased the grain size of cast microstructure.
- As bifilm index was decreased (i.e. higher melt quality), mechanical properties were increased.
- Regardless of Ti grain refinement and Sr modification, there is a good correlation between bifilm index (i.e. melt quality level) and corrosion resistance of A356 alloy. As the bifilm index was decreased, corrosion resistance was increased.
- The  $E_{\text{corr}}$  values for all conditions were determined to be approximately equal, and the samples were pitted rapidly.
- By the degassing of the melt, bifilm index was decreased and the corrosion resistance was increased. The lowest

- [10] Zhang, Y.J., Ma, N.H., Li, X.F. & Wang, H.W., (2014). A new technology to improve the elongation of A356 alloy. in *Solid State Phenomena*. p. 450-454.
- [11] Faraji, M., Eskin, D.G. & Katgerman, L. (2012). Grain refinement in hypoeutectic Al-Si alloys using ultrasonic vibrations. *Foundry Trade Journal International*, 186(3694): range of pages.
- [12] Gnapowski, S., Tsunekawa, Y., Okumiya, M. & Lenik, K., (2013). Change of Aluminum Alloys Structure by Sono-Solidification. *Archives of Foundry Engineering*. 13(4), 39-42.
- [13] Jian, X., Meek, T.T. & Han, Q. (2006). Refinement of eutectic silicon phase of aluminum A356 alloy using high-intensity ultrasonic vibration. *Scripta Materialia*, 54(5): range of pages.
- [14] Jian, X., Xu, H., Meek, T. & Han, Q. (2005). Effect of power ultrasound on solidification of aluminum A356 alloy. *Materials letters*, 59(2): range of pages.
- [15] Li, J.-w., Momono, T., Fu, Y., Jia, Z. & Tayu, Y. (2007). Effect of ultrasonic stirring on temperature distribution and grain refinement in Al-1.65%Si alloy melt. *Transactions of Nonferrous Metals Society of China*, 17(4): range of pages. [http://dx.doi.org/10.1016/S1003-6326\(07\)60158-7](http://dx.doi.org/10.1016/S1003-6326(07)60158-7).
- [16] Łągiewka, M. & Konopka, Z., (2012). The Influence of Material of Mould and Modification on the Structure of AlSi11 Alloy. *Archives of Foundry Engineering*. 12(1), 67-70.
- [17] Tupaj, M., Orłowicz, A.W., Mróz, M., Trytek, A. & Markowska, O., (2016). Usable Properties of AlSi7Mg Alloy after Sodium or Strontium Modification. *Archives of Foundry Engineering*. 16(3), 129-132.
- [18] Zhongwei, C. & Ruijie, Z. (2010). Effect of strontium on primary dendrite and eutectic temperature of A357 aluminum alloy. *Research & Development*: range of pages.
- [19] Campbell, J., (2015). *Complete Casting Handbook: Metal Casting Processes, Metallurgy, Techniques and Design*: Elsevier Science.
- [20] Dispinar, D., Akhtar, S., Nordmark, A., Di Sabatino, M. & Arnberg, L. (2010). Degassing, hydrogen and porosity phenomena in A356. *Materials Science and Engineering: A*, 527(16): range of pages.
- [21] Dispinar, D. & Campbell, J. (2004). Critical assessment of reduced pressure test. Part 2: Quantification. *International Journal of Cast Metals Research*, 17(5): range of pages.
- [22] Dispinar, D. & Campbell, J. (2007). Effect of casting conditions on aluminum metal quality. *Journal of materials processing technology*, 182(1): range of pages.
- [23] Dispinar, D. & Campbell, J. (2011). Porosity, hydrogen and bifilm content in Al alloy castings. *Materials Science and Engineering: A*, 528(10): range of pages.
- [24] Arrabal, R., Mingo, B., Pardo, A., Mohedano, M., Matykina, E. & Rodríguez, I. (2013). Pitting corrosion of rheocast A356 aluminum alloy in 3.5 wt.% NaCl solution. *Corrosion Science*, 73: range of pages.
- [25] Osorio, W.R., Peixoto, L.C., Goulart, P.R. & Garcia, A. (2010). Electrochemical corrosion parameters of as-cast Al-Fe alloys in a NaCl solution. *Corrosion Science*, 52(9): range of pages.
- [26] Park, C., Kim, S., Kwon, Y., Lee, Y. & Lee, J. (2005). Mechanical and corrosion properties of rheocast and low-pressure cast A356-T6 alloy. *Materials Science and Engineering: A*, 391(1): range of pages.
- [27] Dispinar, D., Nordmark, A., Voje, J. & Arnberg, L. (2009). Influence of hydrogen content and bi-film index on feeding behaviour of Al-7Si. in *138th TMS Annual Meeting, Shape Casting: 3rd International Symposium, San Francisco, California, USA, (February 2009)*. (Page Range).